PREPARING THE ASSIMILATION OF IASI -NEW GENERATION IN NWP MODELS: TOWARDS A CHANNEL SELECTION

Francesca Vittorioso, Vincent Guidard, Nadia Fourrié, Javier Andrey-Andrés

PREPARING THE ASSIMILATION OF IASI - NEW GENERATION IN NWP MODELS: TOWARDS A CHANNEL SELECTION

Francesca Vittorioso, Vincent Guidard, Nadia Fourrié, Javier Andrey-Andrés

CNRM UMR 3589, Météo-France & CNRS, GMAP/OBS, Toulouse, France

Abstract

As the EUMETSAT Polar System-Second Generation (EPS-SG) is being prepared, a new generation of the IASI instrument has been designed. The IASI New Generation (IASI-NG) will measure at spectral resolution and a signal-to-noise ratio improved by a factor 2 compared to its predecessor. Measurement precision will be improved as well.

The high amount of data resulting from IASI-NG will present many challenges in the areas of data transmission, storage and assimilation and the number of individual pieces of information will be not exploitable in an operational Numerical Weather Predictions (NWP) context. For these reasons, an appropriate IASI-NG channel selection is going to be performed aiming to select the most informative channels for NWP.

In this paper the propaedeutic study towards a channel selection is displayed. More in details, the construction of a simulated observation database, to be used as a basis for selection, and the use of a diagnostic method to build a full covariance matrix of the observation errors (**R** matrix), will be here described.

INTRODUCTION

The hyperspectral Infrared Atmospheric Sounding Interferometer (IASI), key payload element of the European Meteorological Operational Satellites (MetOp) series, provides since 2007 a huge contribution to Numerical Weather Prediction (NWP), pollution monitoring and climate research.

In the framework of the preparation for the next European polar-orbiting program (EPS-SG), a new generation of the IASI instrument has been designed. The IASI-NG, which will be launched on board the Metop-SG series around 2020, will be characterized by an improvement of both spectral and radiometric characteristics in comparison with IASI. It will measure at 16921 wavelengths (or channels) in each sounding pixel benefiting of a spectral resolution and a signal-to-noise ratio improved by a factor 2 compared to its predecessor [*Crevoisier et al.* (2014)]. Measurement precision will be improved as well starting from the 1 K in temperature and 10% in humidity IASI precision. IASI-NG characteristics will lead to huge improvements in detection and retrieval of numerous chemical species and aerosols, and in thermodynamic profiles retrievals.

The high amount of data resulting from IASI-NG will present many challenges in the areas of data transmission, storage and assimilation. Moreover, the number of individual pieces of information will be not exploitable in an operational NWP context and the choice of an optimal data subset will be needed. For all these reasons, an appropriate IASI-NG channel selection is needed, aiming to select the most informative channels to be used in global and mesoscale NWP models.

The work is being carried out on a simulated observation database, containing simulated data for IASI and IASI-NG. One-dimensional variational (1D-Var) assimilation experiments have been carried out as well in order to evaluate the impact of IASI-NG with respect to IASI on temperature and humidity retrievals.

Additionally, the need to take into account the error correlations among channels has required a study for the evaluation of full **R** matrices. This propaedeutic study is here below described.

OBSERVING SYSTEM SIMULATION EXPERIMENT (OSSE) CONSTRUCTION AND 1D-VAR RETRIEVALS

Four dates in the middle of each season from 2013 have been selected: February the 4th, May the 6th, August the 6th and November the 4th [*Andrey-Andrés et al.* (2017)]. The full IASI orbit for each one of these dates has been computed for a total of 5 242 448 simulations for each instrument (IASI scan geometry is used for IASI-NG).

The experiment has been carried out into four steps: ***(1)*** construction of the input database containing all the required information; ***(2)*** spectra simulation for both IASI and IASI-NG; ***(3)*** data perturbation; ***(4)*** introduction of perturbed input data into 1D-Var.

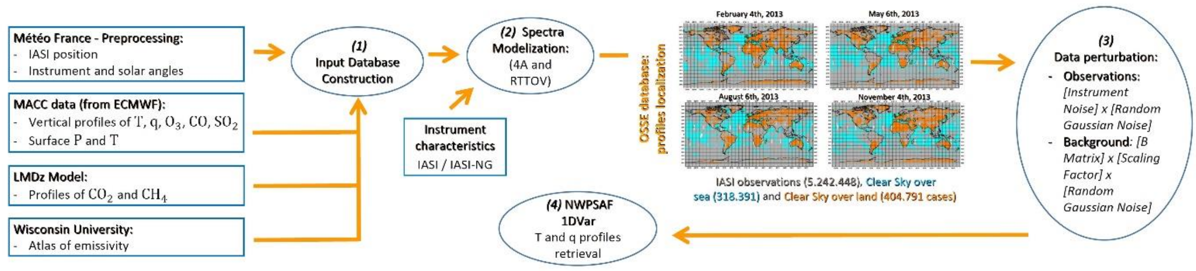

Figure 1: **OSSE database construction stages and 1D-Var retrievals.**

CASE STUDY

In order to undertake the present effort, whose first step has been planned to be carried out on *nadir – over sea – clear sky* conditions, a subset of data has been derived from the starting OSSE database. More in details, 1 099 of the 318 391 observations matching these criteria have been judged to be a representative sample of the overall data. The new subset contains observations for:

- *May and August*
- *polar, mid-latitudes and tropical regions*
- *day and night*

located as in Figure 2.

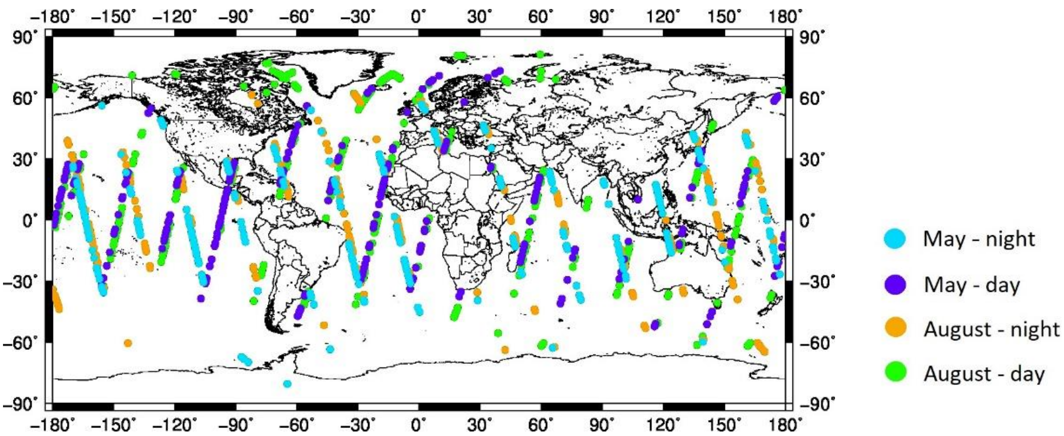

Figure 2: **Subset of selected observations for preparing the IASI-NG channel selection.**

PROPAEDEUTIC STUDY TOWARDS A CHANNEL SELECTION

A series of tests has been carried out on 1D-Var output retrieved profiles to evaluate the behavior of IASI-NG with respect to IASI. For this purpose 123 IASI channels (99 longwave CO_2 channels for temperature, 4 window channels and 20 water vapour channels), already selected at Météo-France in the operational context of the global model ARPEGE, have been used. The 123 IASI-NG corresponding channels at the same central wavenumbers have been taken into account as well for this preliminary study. In this first stage, a diagonal covariance matrix of the observation errors (**R** matrix) filled in with the instrument noise, has been provided as input to the 1D-Var.

Nevertheless, using a diagonal **R** matrix that only contains information about the instrument noise error can be quite unrealistic, since it does not take into account all the other sources of observation errors. This significantly contributes to correlations between different channel errors, which should be taken into account in this kind of study. For this reason, a diagnostic procedure introduced by *Desroziers et al.* (2005) has been used to estimate the structure of the full **R** matrix.

A code has been developed in order to implement the diagnostic until its convergence. Through this tool, the different regions of the spectrum that IASI-NG is able to characterize and therefore the bands in which it is divided, have been explored. The attention has been mainly focused on the BAND 1 and BAND 2 (see Figure 3), which are the most relevant for the assimilation in the NWP context.

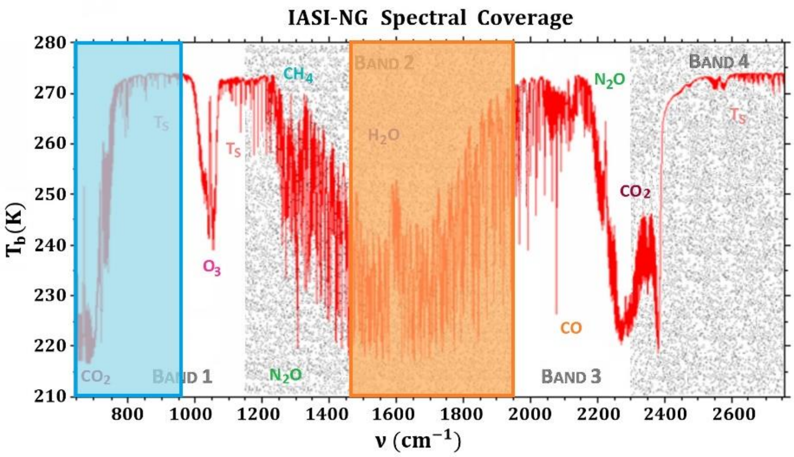

***Figure 3*: here highlighted are BAND 1 (blue) and BAND 2 (orange) portions of the IASI-NG spectrum, which have been examined during this study.**

Successful trials have been performed in the initial part of BAND 1 (645.000 up to 950.875 cm^{-1} **-** first 2448 channels). This spectrum area was approached by applying 8 parallel diagnostic procedures to the same amount of channel groups, of 306 channels each, and obtained by sampling the entire range at a distance of 1 cm^{-1}. Subsequently, using the data thus obtained a quasi-full **R** matrix has been built for the 2448 total amount of channels and then used to reiterate the diagnostics.

Figure 4 shows the diagnostic error Standard Deviations associated at each iteration of the diagnostic procedure up to its convergence, occurring after seven iterations.

For what concerns the correlations among different channel errors, the matrices corresponding to the first and last step in diagnostic show comparable structures, with the same macro-areas of strong correlation coefficient values (Figure 5).

Looking at the 1D-Var retrievals (Figure 6), we can see different behaviors for temperature and humidity statistics computed on the 1099 case study profiles. More in details, the Standard Deviations values for temperature show, on most of the atmospheric column, a difference in the usage of a quasi-full or a full **R** matrix. Between 1 and 0.1 hPa, on the other hand, the improvement in the use of full-diagnosed matrices is rather evident if compared to the other one (just imperceptible changes between full first and last iteration matrices). In terms of humidity, the improvement in results is clear between the surface and 500 hPa. Even in this case, there are no big differences between the first and last iteration in diagnostics.

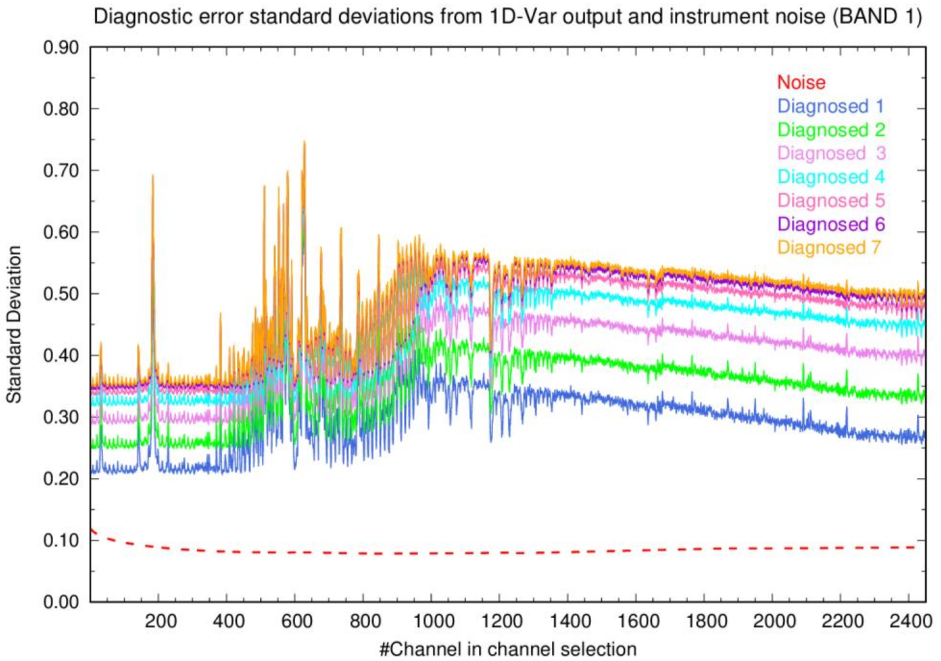

Figure 4: **Diagnosed error Standard Deviations from 1D-Var output and instrument noise for the BAND 1 case.**

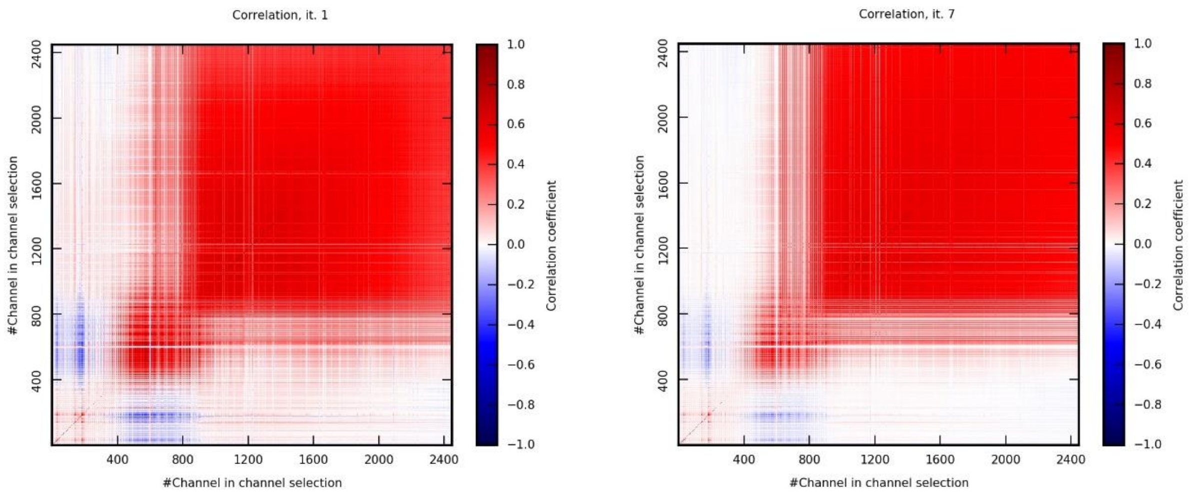

***Figure 5*: BAND 1 diagnostic for correlation matrix from 1D-Var output; first (left) and last or 7th (right) iteration in the process.**

DFS	**Total**	**Temperature**	**Humidity**	**Skin Temp.**
Minimum	6.9	5.1	0.5	0.98
Maximum	10.1	6.0	3.6	1.02
Average	9.0	5.6	2.4	1.00
Median	9.1	5.7	2.4	1.00

Table 1: **DFS values computed for retrieved profiles resulting from the use of the full R matrix from diagnostic convergence (7th) iteration in the 2448 channels of BAND 1.**

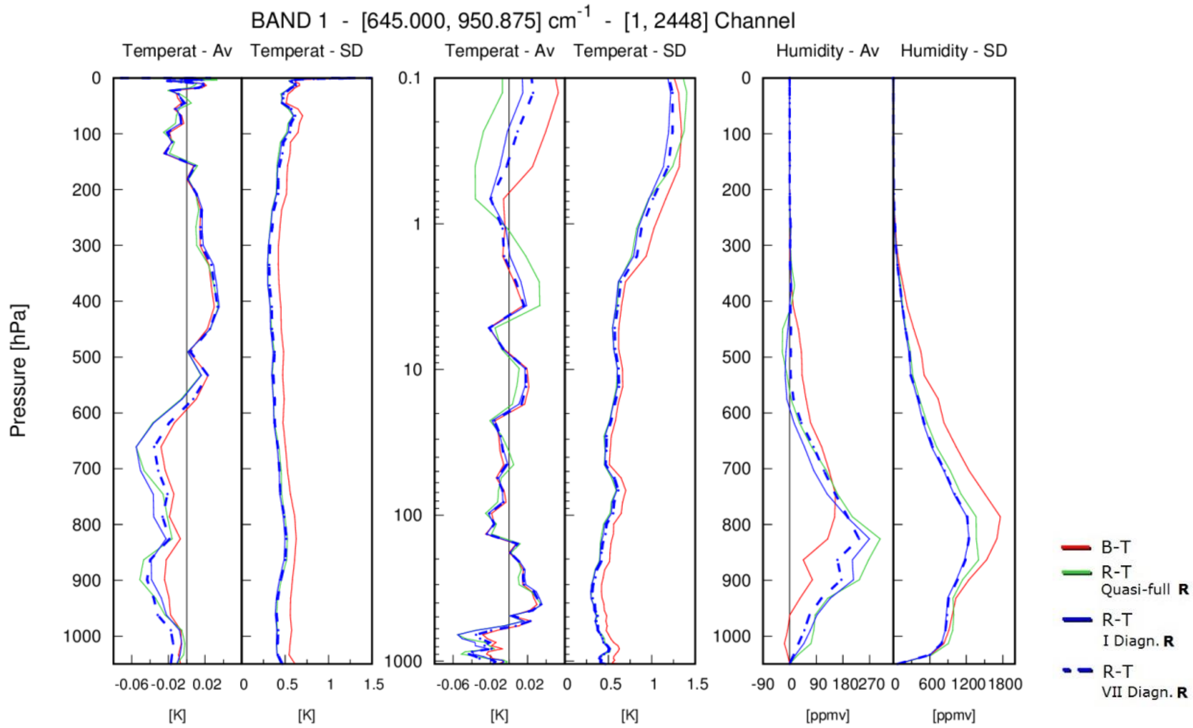

Figure 6: **Background and analysis errors averaged on the 1099 profiles case study, for temperature (linear scale on the left and log scale in the middle) and humidity (right). In each box are Average on the left and Standard Deviation on the right.**

The Degrees of Freedom for the Signal (DFS) has been computed as well. For this purpose, the retrieved profiles resulting from the use of the full **R** matrix from diagnostic convergence iteration (7^{th}) have been used. The results are illustrated in Table 1.

For what concerns BAND 2, the diagnostics has been successfully iterated on a set of 3112 approximately contiguous channels, located in the second half part of the band (1455.000 up to 1950.000 cm^{-1} - channels from 6481 to 10441). The process has been initialized with a diagonal **R** matrix filled in with the instrument noise values.

In this case, we can observe a slower convergence of the diagnostic compared to the previous one (after 10 iterations – Figure 7). The convergence matrix, on the other hand, shows less strong correlations at first iteration if compared to the last one, but always the same kind of structures.

For this part of the study, the 1D-Var has been run using the diagonal **R** matrix, the **R** matrix corresponding to the first iteration of the Desroziers's diagnostic, and the **R** matrix from the last iteration (10^{th}). From the results of the background and analysis errors in Figure 9, we can ascertain a big advantage in the usage of the full 10^{th}-iteration **R** matrix. This improvement is evident in the case of both temperature and humidity Standard Deviations and it is very pronounced if compared to the results coming from a diagonal **R** matrix of instrument noise.

As for BAND 1, the DFS values have been computed as well and are here shown in Table 2.

The Rate of Improvement for Standard Deviations ($Rate\ of\ Improvement = [(R-T)-(B-T)] \cdot (B-T)^{-1}$, where R = Retrievals, B = Background, T = Truth) has been produced for both bands using the 1D-Var output from the use of last Desroziers diagnostic iteration **R** matrices. Figure 10 reaffirms and certifies a good improvement in results. In more details, for what concerns temperature, the improvement is more pronounced for BAND 1, that is the "temperature band". A maximum score is achieved around -0.3. Concerning humidity, on the other hand, the best results are over the 650 hPa (then in the high troposphere) if considering BAND 2 (best results around -0.5 – 450 hPa). The reverse is true in low troposphere, due to the different sensitivity of the involved channels.

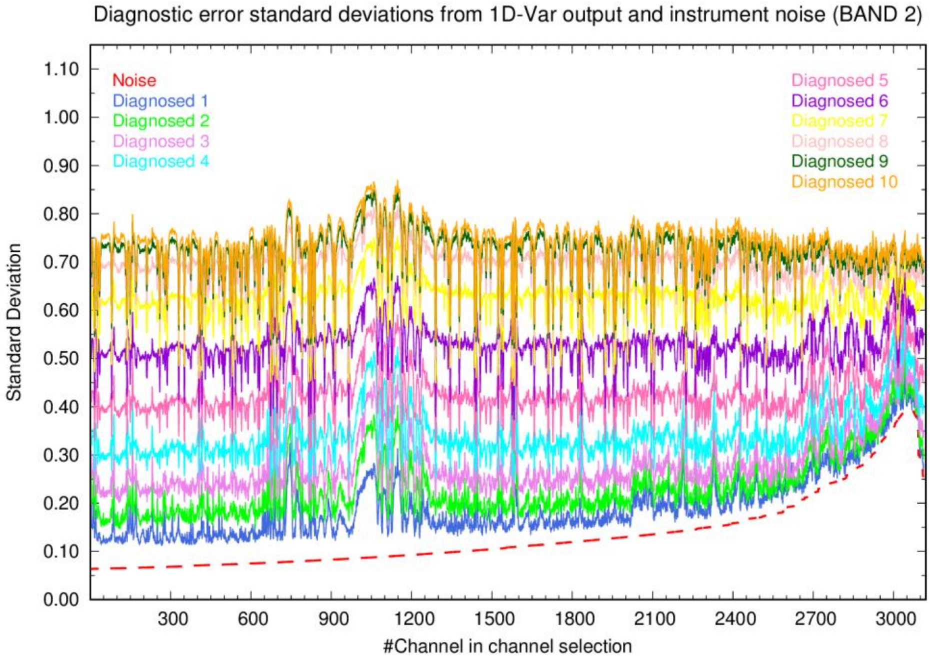

Figure 7: **Diagnosed error Standard Deviations from 1D-Var output and instrument noise for the BAND 2 case.**

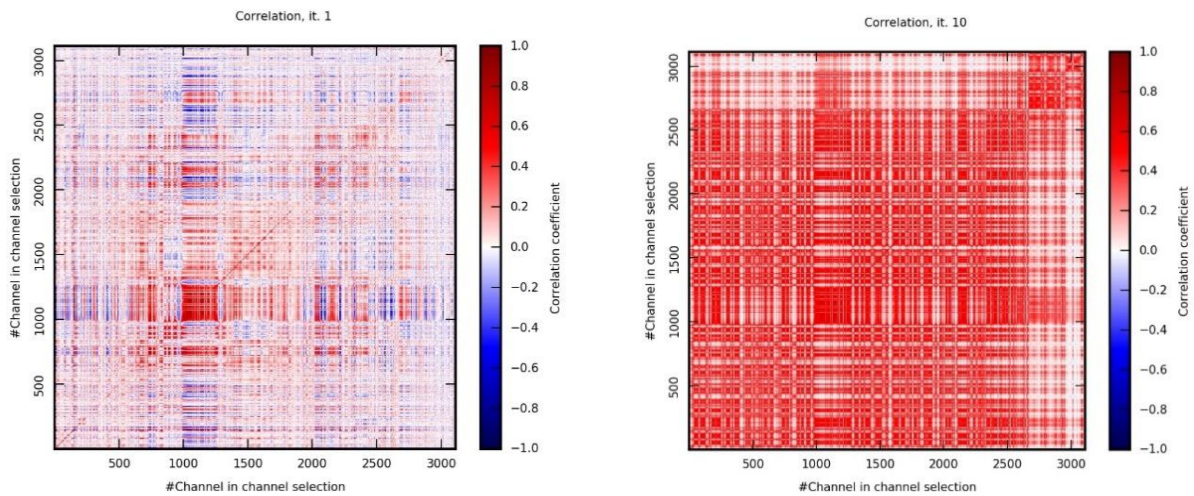

***Figure 8*: BAND 2 diagnostic for correlation matrix from 1D-Var output; first (left) and last or 10th (right) iteration in the process.**

DFS	Total	Temperature	Humidity	Skin Temp.
Minimum	6.4	1.6	3.2	0.09
Maximum	8.7	2.9	6.2	0.97
Average	7.7	2.2	5.0	0.51
Median	7.8	2.2	5.1	0.52

Table 2: **DFS values computed for retrieved profiles resulting from the use of the full R matrix from diagnostic convergence (10th) iteration in BAND 2 (3112 channels).**

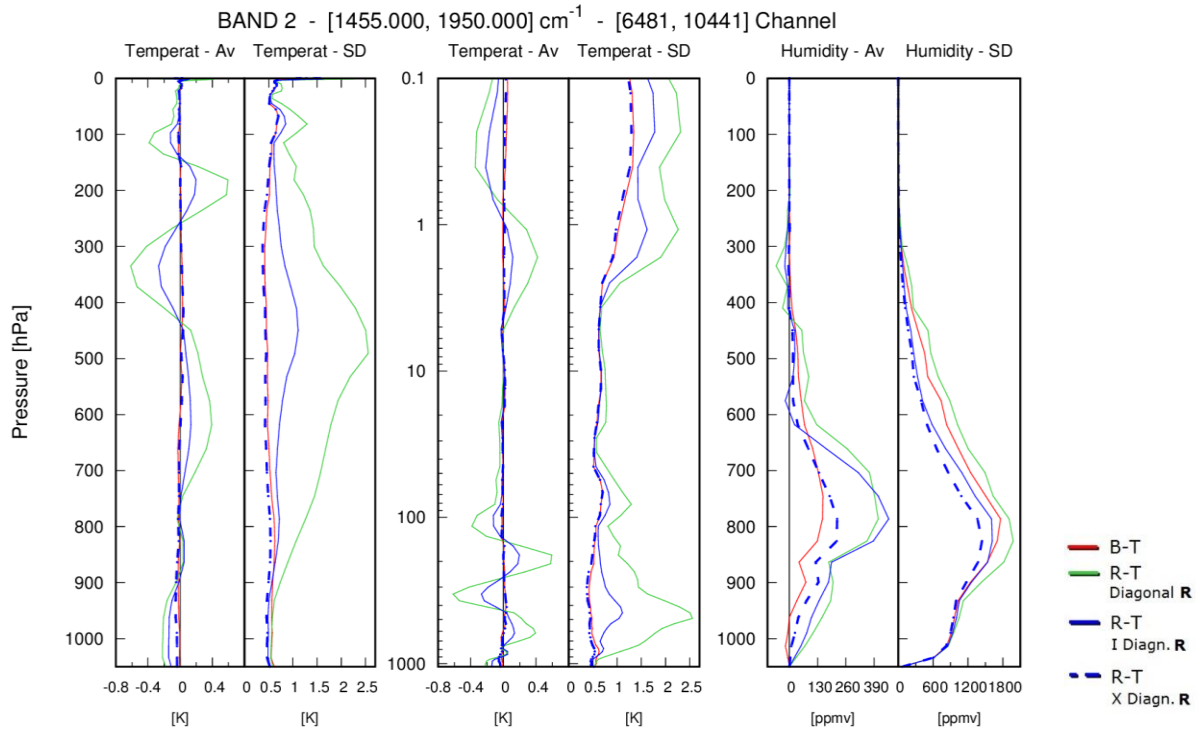

Figure 9: **Background and analysis errors averaged on the 1099 profiles case study, for temperature (linear scale on the left and log scale in the middle) and humidity (right). In each box are Average on the left and Standard Deviation on the right.**

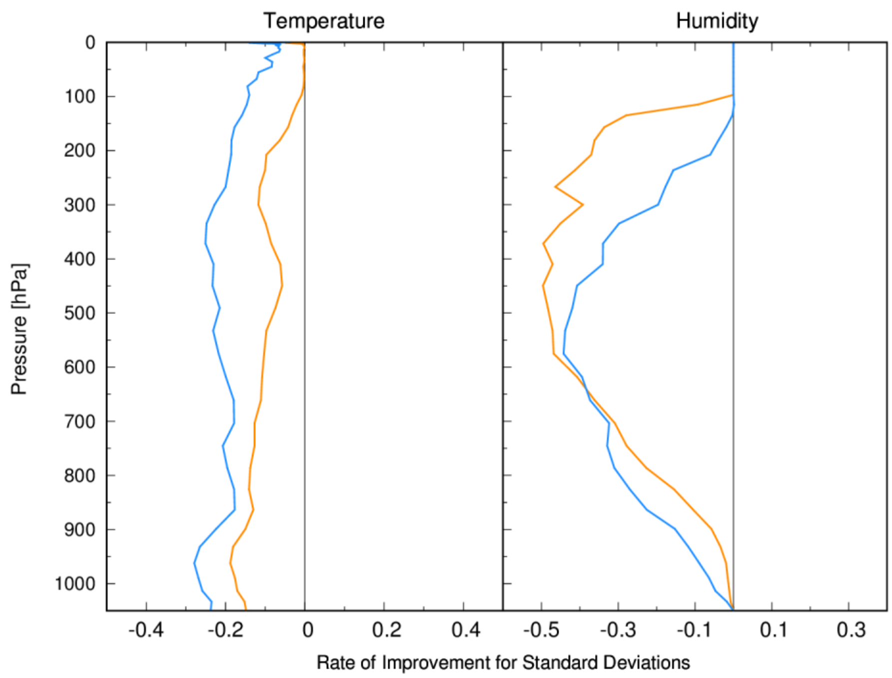

Figure 10**: Rate of Improvement =** $[(R-T)-(B-T)]\cdot(B-T)^{-1}$ **for Standard Deviations (R = Retrievals, B = Background, T = Truth). It has been computed using the results obtained with the last iteration diagnostic matrices.**

FUTURE WORKS: IASI-NG CHANNEL SELECTION FOR THE NWP

The next step in this project will aim at performing an IASI-NG channel selection to be used in operational NWP systems. The selection will be based on a methodology suggested by Rodgers (1996) and proved to be a good *a priori* method for determination of an optimal channel set by Rabier et al. (2002). The method will rely on evaluating the impact of the addition of single channel on a figure of merit. This latter is normally a quantity reflecting the improvement of the analysis error covariance matrix A over the background error covariance matrix B (e.g. DFS or Entropy Reduction – ER).

The selection will be performed on the above-described simulated data and it will rely on sensitivity to geophysical parameters as well as on information content studies.

AKNOWLEDGEMENTS

This research has received funding from the Centre National d'Études Spatiales (CNES) in the framework of the IASI-NG project.

REFERENCES

Andrey-Andrés, J., Fourrié, N., Armante, R., Brunel, P., Crevoisier, C., Guidard, V., and Tournier, B., (2017) A simulated observation database to asses the impact of IASI-NG hyperspectral infrared sounder. Atmos. Meas. Tech. Discussion, **2017**, pp 1-29.

Crevoisier, C., and Coauthors, (2014) Towards IASI-New Generation (IASI-NG): impact of improved spectral resolution and radiometric noise on the retrieval of thermodynamic, chemistry and climate variables. Atmos. Meas. Tech., **7**, pp 4367-4385.

Desroziers, G., Berre, L., Chapnik, B., and Poli, P., (2005) Diagnosis of observation, background and analysis-error statistics in observation space. Q. J. R. Meteorol. Soc., **131**, pp 3385-3396.

Rodgers, C. D., (1996) Information content and optimisation of high spectral resolution measurements. Optical Spectroscopic Techniques and Instrumentation for Atmospheric and Space Research II, SPIE, **2830**, pp 136-147.

Rabier, F., Fourrié, N., Chafai, D., and Prunet, P., (2002) Channel selection methods for Infrared Atmospheric Sounding Interferometer radiances. Q. J. R. Meteorol. Soc., **128**, pp 1011-1027.